

# A Simple Algebraic Grid Adaptation Scheme With Applications to Two- and Three-Dimensional Flow Problems

Andrew T. Hsu  
*Sverdrup Technology, Inc.*  
*NASA Lewis Research Center Group*  
*Cleveland, Ohio*

and

John K. Lytle  
*National Aeronautics and Space Administration*  
*Lewis Research Center*  
*Cleveland, Ohio*

Prepared for the  
9th Computational Fluid Dynamics Conference  
sponsored by the American Institute of Aeronautics and Astronautics  
Buffalo, New York, June 14-16, 1989



(NASA-TM-102446) A SIMPLE ALGEBRAIC GRID  
ADAPTATION SCHEME WITH APPLICATIONS TO TWO-  
AND THREE-DIMENSIONAL FLOW PROBLEMS (NASA)

10 p

CSCL 200

N90-18667

Unclass

G3/34 0266121



# A SIMPLE ALGEBRAIC GRID ADAPTATION SCHEME WITH APPLICATIONS TO TWO- AND THREE-DIMENSIONAL FLOW PROBLEMS

Andrew T. Hsu\*  
Sverdrup Technology, Inc.  
NASA Lewis Research Center Group, Cleveland, Ohio

and

John K. Lytle†  
NASA Lewis Research Center, Cleveland, Ohio

## Abstract

An algebraic adaptive grid scheme based on the concept of arc equidistribution is presented. The scheme locally adjusts the grid density based on gradients of selected flow variables from either finite difference or finite volume calculations. A user-prescribed grid stretching can be specified such that control of the grid spacing can be maintained in areas of known flowfield behavior. For example, the grid can be clustered near a wall for boundary layer resolution and made coarse near the outer boundary of an external flow. A grid smoothing technique is incorporated into the adaptive grid routine, which is found to be more robust and efficient than the weight function filtering technique employed by other researchers. Since the present algebraic scheme requires no iteration or solution of differential equations, the computer time needed for grid adaptation is trivial, making the scheme useful for three-dimensional flow problems. Applications to two- and three-dimensional flow problems show that a considerable improvement in flowfield resolution can be achieved by using the proposed adaptive grid scheme. Although the scheme was developed with steady flow in mind, it is a good candidate for unsteady flow computations because of its efficiency.

## Introduction

The accuracy of numerical solutions in Computational Fluid Dynamics (CFD) is greatly affected by the grid used in the calculation because the discretization error is directly linked to grid sizes in the physical domain. This fact combined with the expanded scale of CFD calculations has produced a need to optimize the use of grid points. Consequently, it is now common practice to use stretched grid, which clusters grid points in regions where gradients (and hence error) are anticipated

to be large. However, in many of the complex problems routinely dealt with by today's CFD researchers, there are often not enough a priori knowledge about the flowfield for one to generate an appropriately stretched grid. In fact, one often finds that a pre-generated grid has clustering in regions that are rather unimportant. For this reason, methods for adapting grids to local flowfield gradients are becoming increasingly popular for improving the accuracy and efficiency of CFD solutions.

In the past decade, many adaptive grid schemes have been developed[1]. These schemes can be divided into two categories. In the first category, partial differential equations (PDE) are solved to generate the grid[2], and in the second category, algebraic relations between the grid sizes and the flow derivatives are solved[3,4]. The advantage of the PDE schemes is that there can be automatic control over the orthogonality and smoothness of the grid, while the advantages of the algebraic schemes are that they are more robust, they are not restricted by boundary point distributions, and they are computationally less time consuming. For these reasons, the algebraic schemes are excellent candidates for unsteady and large three-dimensional flow problems. The use of adaptive grid is especially effective for three-dimensional flow problems for it can drastically reduce the memory and cpu time required for solving a given problem. However, there have been few applications of adaptive grid to three-dimensional flow problems in the past because of the complexity of the methods.

In the present paper, a simple algebraic grid adaptation scheme based on the concept of arc equidistribution is described. The concept of arc equidistribution was first introduced by Dwyer, et al.[3], and had been applied to two-dimensional flow calculations by Gnoffo[5] and later to three-dimensional flow calculations by Nakahashi and Deiwert[4]. The present adaptive grid scheme extends the capability of this basic concept through the addition of a stretching control mechanism and a smoothing procedure.

\*Research Engineer, Member AIAA.

†Aerospace Engineer, CFD Code Assessment Branch, Member AIAA.

One often would like to have an adaptive grid adjust to the flowfield while still retaining certain prescribed stretching. For example, in a flowfield where both a shock and a boundary layer exist, it is difficult for an adaptive grid scheme to capture properly the two high gradient regions simultaneously. This difficulty often results in an insufficient grid distribution in the boundary layer. In external flow calculations, one would like to have a smooth stretching that provides coarse grids near the outer boundary. However, adaptive grid schemes usually give a fairly uniform grid spacing throughout the low gradient regions. These difficulties are fairly common for many of the adaptive grid schemes currently used.

To resolve this problem, the present scheme is so designed that it has the capability of maintaining a prescribed stretching while adapting the grid according to the flow variables, thus allowing the fine grid in a boundary layer and the coarse grid near the outer boundary to remain intact. This unique feature provides the user with additional control on how the grid is to be adapted based on prior knowledge of the flowfield.

For all algebraic adaptive grid schemes, the control of smoothness and orthogonality is a major task. Many sophisticated techniques had been developed by researchers. For instance, Gnoffo[5] used a filtering scheme on the weight function, and Nakahashi and Deiwert [4] used a torsion coefficient to control the smoothness and orthogonality. In the present work, instead of trying to build in sophisticated smoothing schemes, an elliptic smoother is applied after the grid has been adapted. This technique not only simplifies the formulation of the adaptive grid scheme, but also provides the user with greater freedom on the control of smoothness.

In the following sections, the formulation of the adaptive grid scheme is described along with results from applying the scheme to two- and three-dimensional compressible flow problems. The examples consist of a two-dimensional supersonic compression ramp, a two-dimensional hypersonic nozzle and a three-dimensional subsonic jet-in-crossflow. The merits of the scheme are clearly evident through comparisons between calculations using adapted and unadapted grids.

### Adaptive Grid Formulation

The basic idea behind an arc equidistribution scheme is to require the grid size to be inversely proportional to a weight function so that the weight function is equally distributed over the grid points. When the weight function is constructed using the gradient of the flow variables, one would have dense grid distribution in regions of high gradients and thus reduce the discretization errors in these regions. Such rearrangement of the grid will provide a more uniform error distribution, and hence a smaller overall discretization error.

To illustrate this idea, we can write in the  $x$ -direction

$$\Delta x_i w_i = C, \quad (1)$$

where  $\Delta x_i$  is the grid size,  $w_i$  is a weight function that can be constructed using the gradient of any of the flow variables, and  $C$  is a constant. For a general coordinate system  $(\xi, \eta)$ , one can rewrite eq. (1) in the  $\xi$ -direction as:

$$S_\xi w = C \quad (2)$$

where  $S$  is the arc length on an  $\eta = \text{const}$  line. Anderson[2] derived a system of partial differential equations for the  $x, y$  coordinates based on equation (2). In the present work, eq. (2) is used directly to derive the necessary algebraic relations for grid adaptation.

Since it is customary to use  $\Delta \xi = 1$  in the computational domain, equation (2) can be cast into the following discretized form:

$$\Delta S_i w_i = \lambda C_i \quad (3)$$

where

$$\Delta S_i = [(x_{i+1} - x_i)^2 + (y_{i+1} - y_i)^2]^{1/2} \quad (4)$$

and

$$w_i = 1 + \beta \left| \frac{\partial u}{\partial \xi} \right|_i \quad (5)$$

with  $u$  representing any of the flow variables and  $\beta$  a constant that controls the sensitivity to the flow gradient. The coefficient  $\lambda$  is a constant to be determined, and  $C_i$  can either be a constant or a function of  $\xi$ . If one chooses

$$C_i = \Delta S_i^0, \quad (6)$$

with  $\Delta S_i^0$  being the arc length of the old grid spacing, the scheme will have "memory," i.e., it will have the ability to retain the old spacing in the absence of strong gradients in  $u$ . If  $C_i$  is a user prescribed function of  $\xi$ , be it a polynomial or an exponential function, then the resulting adaptive grid will keep this prescribed stretching while also adapting the grid spacing in accordance with the flow gradient. This feature of stretching control will be illustrated later in the Results and Discussion Section.

The constant  $\lambda$  can be determined by requiring the new total arc length to be the same as the old total arc length, i.e.,

$$\sum_i \Delta S_i^0 = \sum_i \Delta S_i = \lambda \sum_i \frac{C_i}{w_i} \quad (7)$$

Solving the above equation for  $\lambda$  yields

$$\lambda = \frac{\sum_i \Delta S_i^0}{\sum_i \frac{C_i}{w_i}} \quad (8)$$

Now, assume that the boundary coordinates  $(x_1, y_1)$  are given, and the grid spacing along one  $\eta = \text{const}$  line has been calculated from eq. (3), then one can determine  $x_{i+1}$  and  $y_{i+1}$  from known values of  $x_i, y_i, \Delta S_i$ , and the old coordinates  $x_i^0$  and  $y_i^0$ . We assume that the new grid point is located on the same  $\eta = \text{const}$  line. Define the arc lengths as

$$S_i = \sum_{k=1}^i \Delta S_k, \quad (9)$$

$$S_i^o = \sum_{k=1}^i \Delta S_k^o. \quad (10)$$

If

$$S_n^o \leq S_i \leq S_{n+1}^o \quad (11)$$

where  $n$  is the index of the old arc lengths, then we require  $x_{i+1}$  and  $y_{i+1}$  to satisfy

$$y = a_n x + b_n, \quad (12)$$

where

$$a_n = \frac{y_{n+1}^o - y_n^o}{x_{n+1}^o - x_n^o} \quad (13)$$

$$b_n = \frac{y_n^o x_{n+1}^o - y_{n+1}^o x_n^o}{x_{n+1}^o - x_n^o}. \quad (14)$$

With these formulations, the new coordinates can now be solved from eqs. (4) and (12). If we always keep the last grid point on the boundary, then no iteration is needed in the calculation.

For a simple mesh, that is for a grid mesh wherein all the grid lines do not deviate significantly from the  $x$ - and  $y$ -directions, one can replace  $\Delta S_i$  in equation (3) by  $\Delta x_i$  or  $\Delta y_i$ , then  $x_i$  and  $y_i$  can be obtained directly from

$$x_i = x_{i-1} + \Delta x_i, \quad y_i = y_{i-1} + \Delta y_i, \quad (15)$$

and there is no need to solve equations (4) and (12), making the process simpler. Simple mesh is a frequent occurrence in internal flow computations.

Since the above described adaptive grid procedure is basically an algebraic system solved on a line-by-line basis, there is no control over the smoothness or the orthogonality of the resulting grid. In the present work, instead of trying to build sophisticated control features into the scheme, a simple elliptic smoother is used to achieve the same end after the grid has been adapted. For example, for the  $y$ -coordinate one can use either a simple two point averaging

$$y_i = \frac{1}{2}(y_{i+1} + y_{i-1}), \quad i = 2, 3, 4, \dots \quad (16)$$

or a four point averaging

$$y_{i,j} = \frac{1}{4}(y_{i+1,j} + y_{i-1,j} + y_{i,j+1} + y_{i,j-1}), \quad i, j = 2, 3, 4, \dots \quad (17)$$

This smoothing process can be applied to the adapted grid as many times as one chooses to achieve the desired smoothness. Two or three iterations through the smoothing process is often enough in practice. This is called an elliptic smoother because equation (17) is, in fact, the discretized form of a Laplace equation, and the averaging process is equivalent to solving the equation  $y_{\xi\xi} + y_{\eta\eta} = 0$  iteratively.

During the grid adaptation process, the boundary points can either be fixed or floating, depending on the user's intention. When letting the boundary points float, one can either use the above formula to adapt the boundary grid points or simply use extrapolations from interior points.

## Results and Discussions

A number of two- and three-dimensional flow problems have been studied using the above described adaptive grid scheme. Since at this time we are only concerned with steady flow problems, a stand alone adaptive grid routine that can be used with various finite difference or finite volume flow solvers was developed. The adaptive grid routine reads grid and flow variables from the output of a flow solver, generates the flow-adapted grid, and interpolates the flow variables on the new grid. The new grid and flow variables are then used by the flow solver to continue the computation. A typical adaptive solution would need two to three iterations between the flow solver and the grid adaptation routine.

The flow solvers used in the present work are the PARC2D and PARC3D codes[4], that were originally developed by NASA Ames[5] and modified by the AEDC Group of Sverdrup Technology, Inc. for internal flow problems. These codes solve the full Navier-Stokes equations using the approximate factorization algorithm by Beam and Warming[6]. Central differences are used in discretizing the spatial derivatives, and backward differences are used for the time derivatives. To avoid having to solve a block pentadiagonal matrix, the Jacobian matrices are diagonalized using their eigenvalues and eigenvectors. This procedure results in a set of scalar pentadiagonal equations. Second-order and forth-order artificial dissipation terms are used in the code to ensure stability and convergence.

### Supersonic Ramp Flow

In order to illustrate the ability of the present scheme to maintain a prescribed grid stretching and the effect of the elliptic smoother, a supersonic viscous flow over a 9.5 degree ramp was computed. The initial solution and the unadapted grid used for the initial computation is shown in Figure 1 and 2. The freestream Mach number is 3, and the Reynolds number is  $1 \times 10^6$ . A  $46 \times 45$  grid is used.

Without the new feature of stretching control, i.e., with  $C_i$  in equation (3) being a constant, the adaptive grid scheme generated a grid as shown in Figure 3, which pushed the grid points towards the upper boundary and left only a few points for the boundary layer. The condition persisted despite the use of various combinations of flow variables in constructing the weight function.

This problem was then solve with the stretching control feature. The coefficients  $C_i$  were given as  $C_{i+1} = 1.1C_i$ , which is the original stretching for the initial unadapted grid shown in Figure 2. Figure 4(a) shows that by using the new scheme the desired fine grid for the

boundary layer is retained, while a finer grid for shock capturing is also provided.

The grid lines in Figure 4a exhibit some kinks and the changes in grid spacing are abrupt. Both characteristics were eliminated by application of the elliptic smoother as shown in Figure 4(b). In this specific case, the grid had been run through the smoother five times.

The final adaptive solution is given in Figure 5 as the flowfield Mach contours. The Mach contours show that the diffused shock in the initial solution (Figure 1) is now replaced by a sharp shock in the adaptive solution.

#### Hypersonic Nozzle Flow

The next application we present is a two-dimensional adaptive computation of a generic hypersonic nozzle for the National Aero-Space Plane. The geometry is shown in Figure 6(a). The freestream Mach number is 3, the combustor exit Mach number is 1, and pressure ratio between the combustor exit and the freestream is 7, the Reynolds number based on the velocity at, and the height of, the combustor exit is  $1.09 \times 10^6$ , and turbulent flow is assumed. The Mach number contours of this flowfield are shown in Figure 6(b). Under the above condition, the nozzle flow is overexpanded. The shear layer trailing the cowl, between the freestream and the engine exhaust, is bent towards the upper solid wall due to the higher freestream pressure. The turning of the flow at the cowl lip causes a shock which reaches the upper wall and is reflected. Thus the flowfield contains boundary layers, free shear layers, and shocks, making it difficult to cluster grid points in the high gradient regions before knowing the solution.

A flow adapted grid, shown in Figure 7, is first obtained by using constant  $C_i$  in equation (3). The clustering of the grid clearly shows the positions of the free shear layer and the oblique shock above the free shear layer, and it is apparent that a pre-generated grid cannot provide the necessary fine grid for these high gradient regions. The finer grid in the free shear layer region produces a better resolution for the mixing between the engine exhaust and the external air, an important phenomenon in high speed flight. However, grid lines have been pulled away from the solid surface by the strong gradients in the shock and the free shear layer, as can be observed from Figure 7(b), which is a magnified part of the grid near the upper wall. The very coarse grid at the boundary could cause larger errors in shear stress and heat transfer predictions at the wall. This problem is common to many adaptive grid schemes presently in use (see e.g., Ref. [7]).

The boundary resolution problem is successfully resolved in the present study by assigning  $C_i$  in equation (3) a function of  $y$ . An adapted grid that preserves a prescribed stretching is shown in Figure 8. In this grid, a reasonably fine grid spacing is maintained at the boundary, ensuring better resolution at the solid wall.

A comparison between the pressure distributions on the upper wall of the nozzle before and after the use of the adapted grid is given in Figure 9. From this comparison we observe that without adaptive grid, the oblique shock is rather diffuse before it reaches the upper wall, thus producing a smeared pressure distribution on the wall. On the other hand, the adaptive grid result not only has moved the position of the shock slightly downstream, but also gives a steeper pressure rise at where the shock reaches the wall. These differences in pressure distributions will, of course, directly affect the numerical prediction of the nozzle performance.

Note that in the present case, grid adaptation in only one direction is sufficient; in fact, this is true for many circumstances. However, to illustrate the capability of treating three-dimensional flow problems with the present scheme, the following example of circular jet injection is presented where grid adaptation is done in all three directions.

#### Three-dimensional Jet-in-crossflow

The three-dimensional version of the adaptive grid scheme was tested on a compressible subsonic jet-in-crossflow problem. Interest in this case originates from applications to combustion, film cooling, thrust vector control jets, propulsive jets and ejectors. Previous investigators [8,9] have found these problems to be grid dependent even on grids as dense as  $98 \times 82 \times 62$ . It is obviously impractical to routinely obtain solutions on grids of this size when using a full Navier-Stokes code such as PARC3D. Consequently, the adaptive grid scheme was applied to the jet-in-crossflow problem with a moderate grid density of  $50 \times 40 \times 30$  to illustrate its effect on the distribution of grid points and on the jet trajectory.

The conditions selected for this study were a jet injected at 90 degrees to the crossflow with a velocity ratio between the jet and crossflow,  $U_j/U_\infty$ , of 4.0. A schematic representation of this case is shown in Figure 10. To minimize the computational effort, only one-half of the flowfield was solved by assuming symmetry along the X-Y plane. In addition, a slip-wall condition was imposed along the boundary containing the jet orifice.

Solutions were obtained with the PARC3D code using two different grids of the same overall density,  $50 \times 40 \times 30$  ( $X \times Y \times Z$ ). The first calculation was performed on an unadapted grid with uniform spacing except near the jet where the spacing was reduced to resolve the jet orifice. The second calculation was started by adapting this grid to local gradients in the total velocity. The location of boundary points was determined by extrapolation from the computational domain except along the boundary containing the orifice where the points remained fixed. In addition, no grid stretching was prescribed.

The results from the unadapted and adapted grid

solutions are represented in Figure 11 (a) and 11 (b), respectively, by Mach number contours along the center-plane. The effect of grid adaptation is apparent in the redistribution of grid points in Figure 11 (b). Points are clustered on the aft side of the jet where strong gradients exist between the jet and wake. Outside of the jet interaction region, where no significant gradients are present, the grid points are uniformly distributed. A direct result of grid adaptation on the flowfield is evident in the difference in jet penetration between the two cases. Greater resolution of the jet-wake region in the adapted grid case results in less jet penetration which is in better agreement with the data of Fearn and Weston [10] than the result from the unadapted grid case.

A detailed comparison with experimental data will be made after the boundary layer is resolved using the grid stretching control feature of the adaptive grid scheme. A comparison of three-dimensional grids generated with and without this feature are shown in Figure 12 (a) and (b), respectively. The axes of both grids are centered at the jet orifice. Figure 12 (b) is from the case described above in which no stretching was prescribed. As a result, the grid spacing becomes uniform away from the jet. For the case shown in Figure 12 (a), stretching was prescribed in the Y-direction to resolve the boundary layer and in the X- and Z-directions to resolve the jet orifice. Notice that the stretching is preserved in all three directions, even away from the jet.

The adapted grid generated for the three-dimensional case was skewed near the jet which initially caused concern regarding the rate of convergence to a solution. However, the convergence history for the adapted grid solution was comparable to the unadapted grid solution. The residual was reduced approximately eight orders of magnitude in two thousand iterations in both cases.

### Conclusions

An adaptive grid scheme that has the ability of retaining a prescribed stretching has been developed on the basis of the arc equidistribution concept. The combination of this scheme with an elliptic smoother produces a computationally efficient adaptive grid. The scheme has been successfully applied to both two- and three-dimensional flow computations, and the numerical results show significant improvements in flowfield resolution.

### Acknowledgement

This work is partially supported by the NASA Lewis Research Center under Contract NAS3-25266 with Dr. M.-S. Liou as monitor. Parts of the computations are performed on the NAS computers at NASA Ames.

### References

1. Advances in Grid Generation, K. N. Ghia and U. Ghia, Editors, ASME, June 1983.
2. Anderson, D.A. and Steinbrenner, J., "Generating Adaptive Grids with a Conventional Grid Scheme." AIAA Paper 86-0427.
3. Dwyer, H., Kee, R. and Sanders, B., "Adaptive Grid Method for Problems in Fluid Mechanics and Heat Transfer," AIAA Journal, Vol. 18, Oct. 1980.
4. Nakahashi, K. and Deiwert, G.S., "Adaptive Grid Method with Application to Airfoil Flow." AIAA Journal, Vol. 25, No. 4, April 1987, pp. 513-520.
5. Gnoffo, P.A., "A Vectorized, Finite Volume, Adaptive Grid Algorithm for Navier-Stokes Calculations," Numerical Grid Generation, J.F. Thompson, editor, Elsevier Science Publishing Co., Inc., 1982, pp. 819-835.
6. Nakahashi, K. and Deiwert, G.S., "A Three-Dimensional Adaptive Grid Method," AIAA Paper 85-0486, January 1985.
7. Baysal, O., Englund, W.C., Eleshaky, M.E. and Pittman, J.L., "Adaptive Computations of Multispecies Mixing Between Scramjet Nozzle Flows and Hypersonic Freestream," AIAA Paper 89-0009, January 1989.
8. Harloff, G.J., and Lytle, J.K., "Three-dimensional Viscous Flow Computations of a Circular Jet in Subsonic and Supersonic Cross Flow," 1st National Fluid Dynamics Congress, July 25-28, 1988, Cincinnati, Ohio.
9. Roth, K.R., Fearn, R.L. and Thakur, S.S., "A Numerical Study of the Contrarotating Vortex Pair Associated with a Jet in a Crossflow," AIAA-89-0448.
10. Fearn, R.L. and Weston, R.P., "Velocity Field of a Round Jet in a Crossflow for Various Jet Injection Angles and Velocity Ratios," NASA Technical Paper 1506, October 1979.

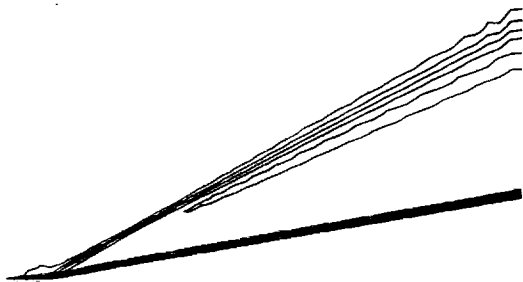


Figure 1. The Mach number contours of an unadapted grid solution for a Mach 3 viscous flow over a 9.5 degree ramp.

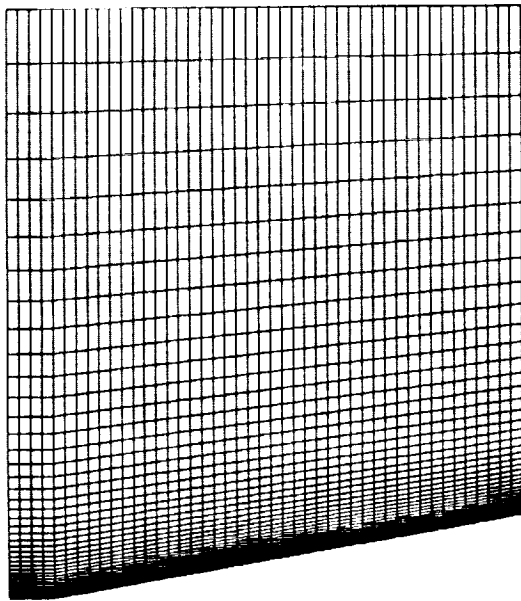


Figure 2. The initial grid used for the supersonic flow over a ramp.

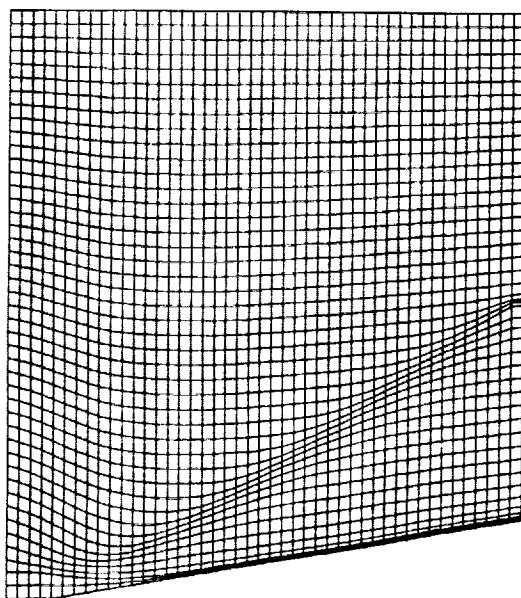


Figure 3. The adapted grid without prescribed stretching.

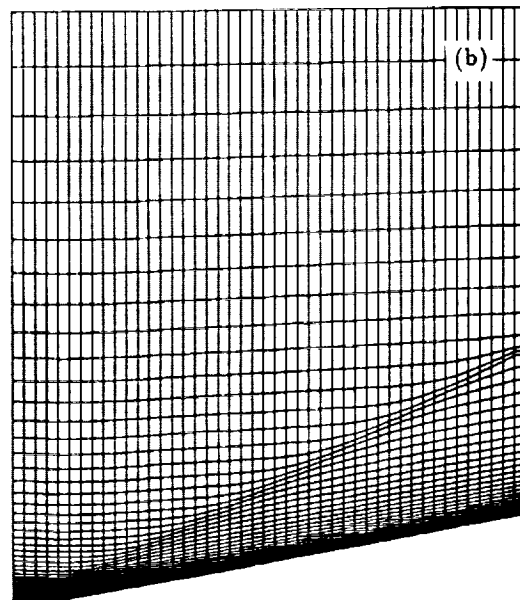
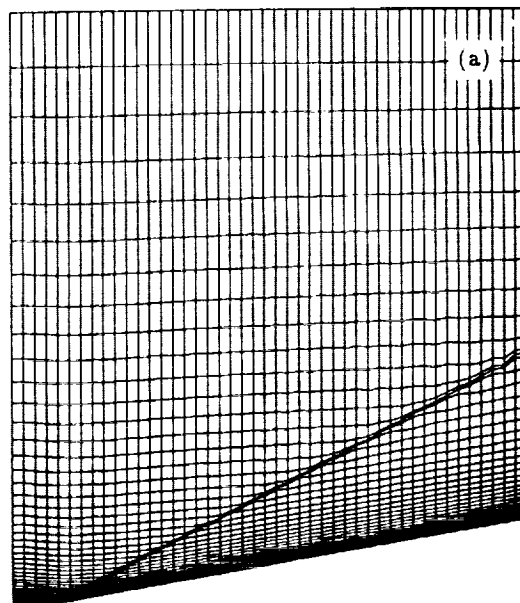


Figure 4. The adapted grid with prescribed stretching: (a) without smoothing, (b) with smoothing.



Figure 5. The adapted grid solution for the supersonic ramp flow; Mach number contours.



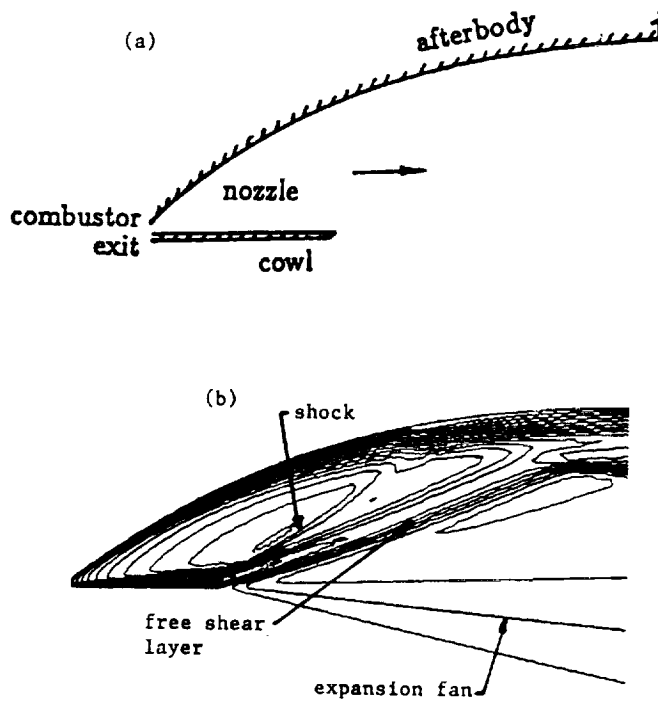


Figure 6. Schematic representation of a hypersonic nozzle, and the Mach number contours of the flowfield.

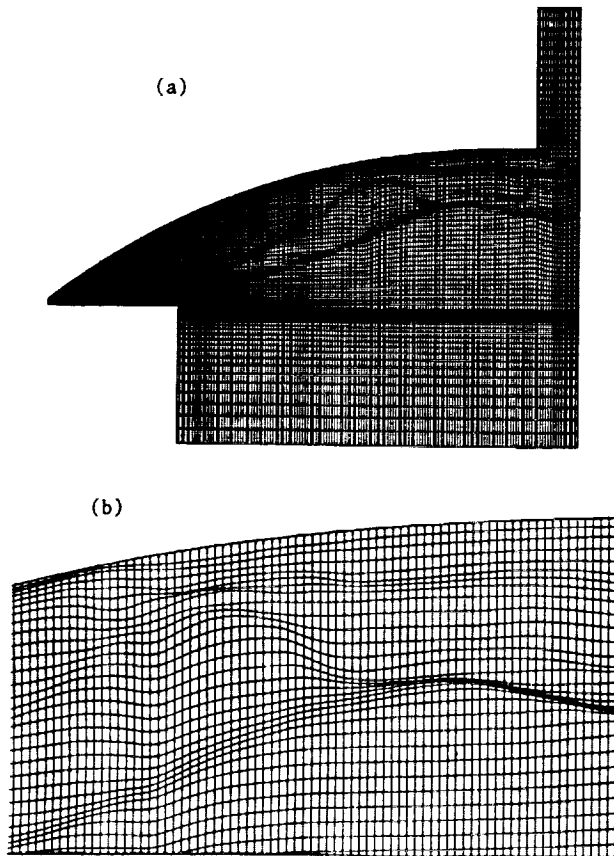


Figure 7. The adapted grid for the hypersonic nozzle flow,  $C_i = \text{const.}$  (a) complete grid, (b) magnified view of the upper wall near the shock.

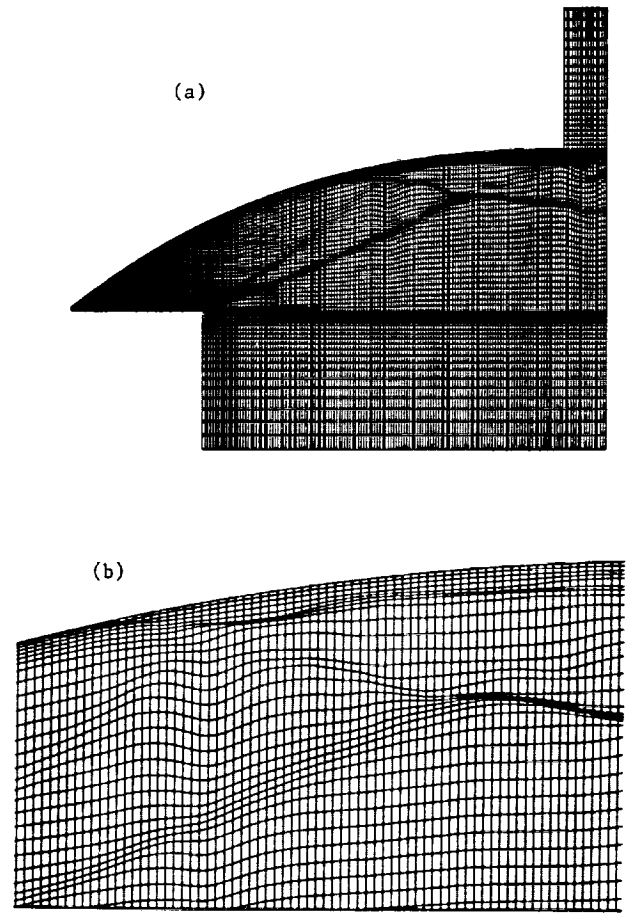


Figure 8. The adapted grid for the hypersonic nozzle flow,  $C_i = f(y)$ . (a) complete grid, (b) magnified view of the upper wall near the shock.

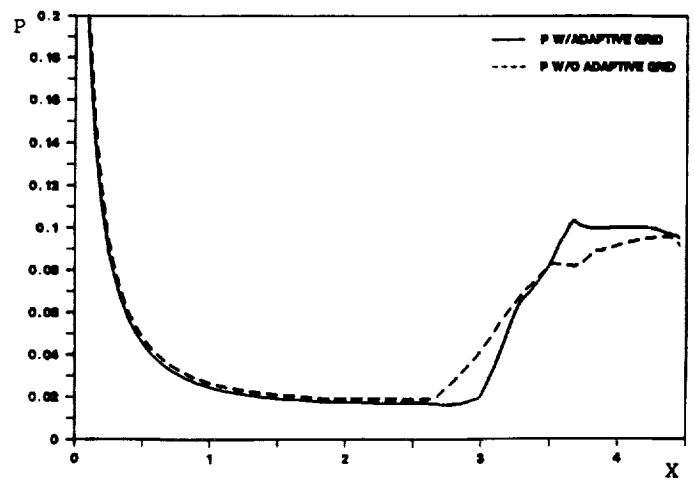


Figure 9. Comparison of pressure distributions on the upper nozzle wall.

ORIGINAL PAGE IS  
OF POOR QUALITY

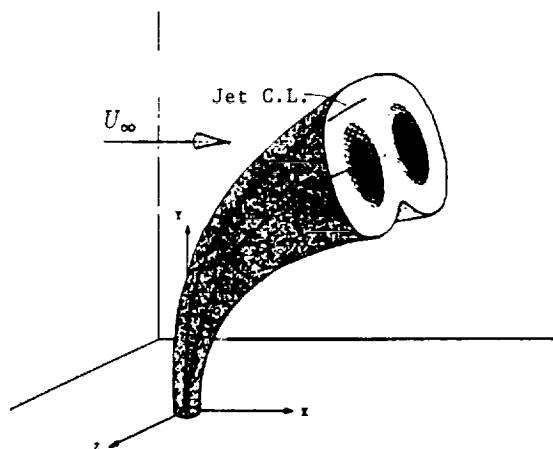


Figure 10. Schematic representation of a jet-in-cross flow.

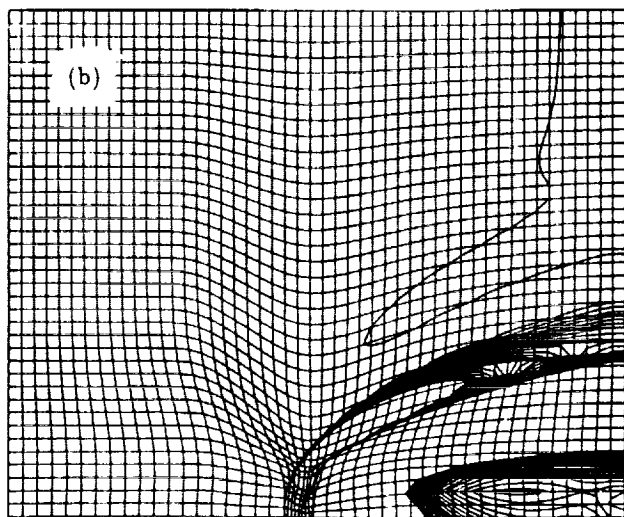
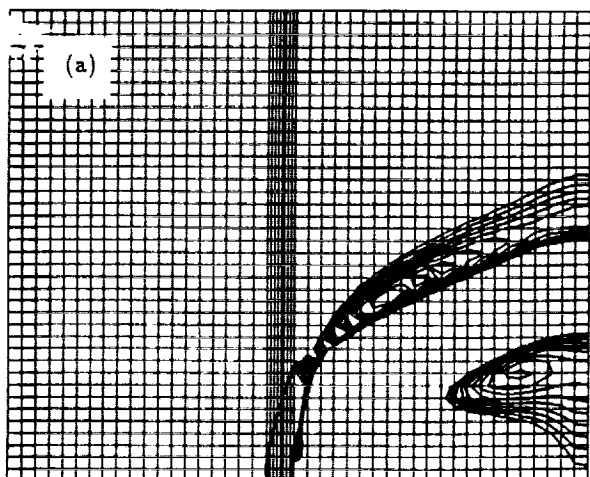


Figure 11. Mach number contours on centerplane;  $U_j/U_\infty = 4.0$ ,  $50 \times 40 \times 30$  grid. (a) unadapted grid solution. (b) adapted grid solution.

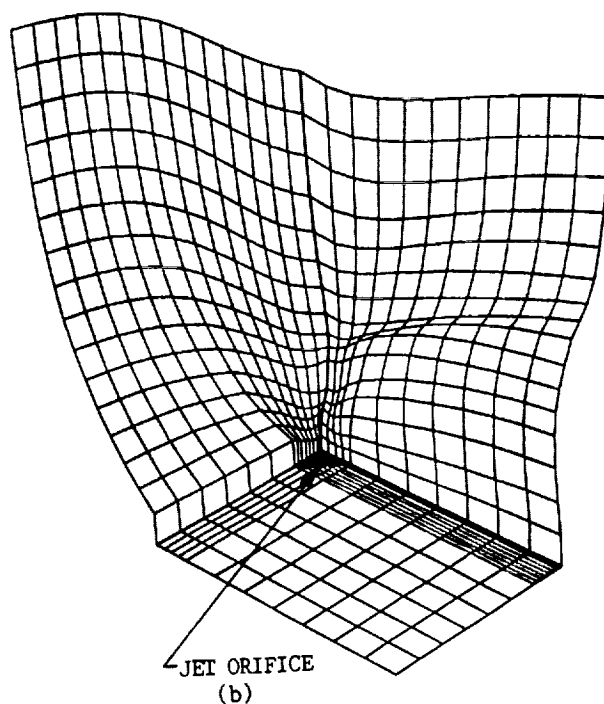
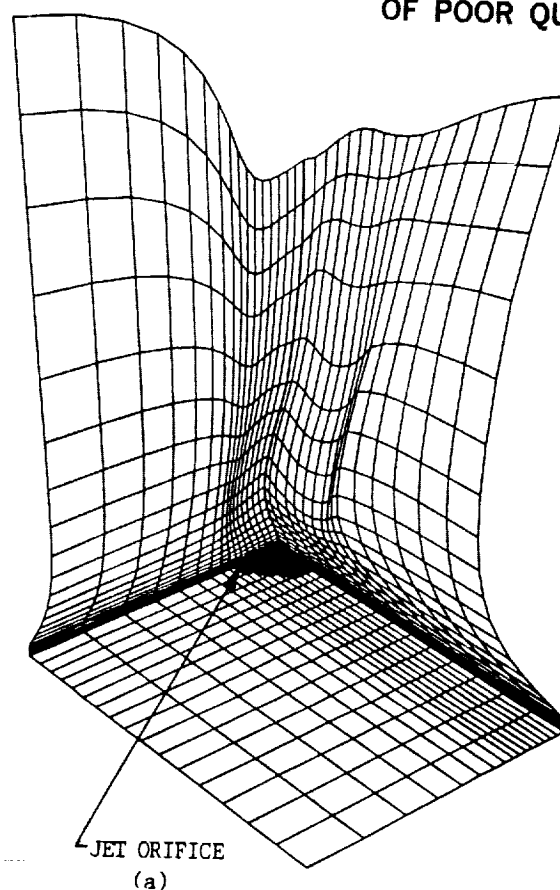


Figure 12. Three-dimensional adapted grid for the jet-in-crossflow problem; (a) stretched grid, (b) un-stretched grid.

# Report Documentation Page

1. Report No. NASA TM-102446		2. Government Accession No.		3. Recipient's Catalog No.	
4. Title and Subtitle A Simple Algebraic Grid Adaptation Scheme With Applications to Two- and Three-Dimensional Flow Problems				5. Report Date	
				6. Performing Organization Code	
7. Author(s) Andrew T. Hsu and John K. Lytle				8. Performing Organization Report No. E-5229	
				10. Work Unit No. 505-62-21	
9. Performing Organization Name and Address National Aeronautics and Space Administration Lewis Research Center Cleveland, Ohio 44135-3191				11. Contract or Grant No.	
				13. Type of Report and Period Covered Technical Memorandum	
12. Sponsoring Agency Name and Address National Aeronautics and Space Administration Washington, D.C. 20546-0001				14. Sponsoring Agency Code	
15. Supplementary Notes Prepared for the 9th Computational Fluid Dynamics Conference sponsored by the American Institute of Aeronautics and Astronautics, Buffalo, New York, June 14-16, 1989. Andrew T. Hsu, Sverdrup Technology, Inc., NASA Lewis Research Center Group, Cleveland, Ohio 44135; John K. Lytle, NASA Lewis Research Center.					
16. Abstract An algebraic adaptive grid scheme based on the concept of arc equidistribution is presented. The scheme locally adjusts the grid density based on gradients of selected flow variables from either finite difference or finite volume calculations. A user-prescribed grid stretching can be specified such that control of the grid spacing can be maintained in areas of known flowfield behavior. For example, the grid can be clustered near a wall for boundary layer resolution and made coarse near the outer boundary of an external flow. A grid smoothing technique is incorporated into the adaptive grid routine, which is found to be more robust and efficient than the weight function filtering technique employed by other researchers. Since the present algebraic scheme requires no iteration or solution of differential equations, the computer time needed for grid adaptation is trivial, making the scheme useful for three-dimensional flow problems. Applications to two- and three-dimensional flow problems show that a considerable improvement in flowfield resolution can be achieved by using the proposed adaptive grid scheme. Although the scheme was developed with steady flow in mind, it is a good candidate for unsteady flow computations because of its efficiency.					
17. Key Words (Suggested by Author(s)) CFD Adaptive grid			18. Distribution Statement Unclassified - Unlimited Subject Category 34		
19. Security Classif. (of this report) Unclassified		20. Security Classif. (of this page) Unclassified		21. No. of pages 10	
				22. Price* A02	

